SUPPLEMENTAL INFORMATION

Acetyl-CoA synthetase 2: a critical linkage in obesity-induced tumorigenesis in myeloma

Zongwei Li, Huan Liu, Jin He, Zhiqiang Wang, Zheng Yin, Gichun You, Zhiming Wang, Richard E. Davis, Pei Lin, P. Leif Bergsagel, Elisabet E. Manasanch, Stephen T.C. Wong, Nestor F. Esnaola, Jenny C. Chang, Robert Z. Orlowski, Qing Yi, and Jing Yang

Supplementary Figures

Supplementary Tables

Supplementary Figures

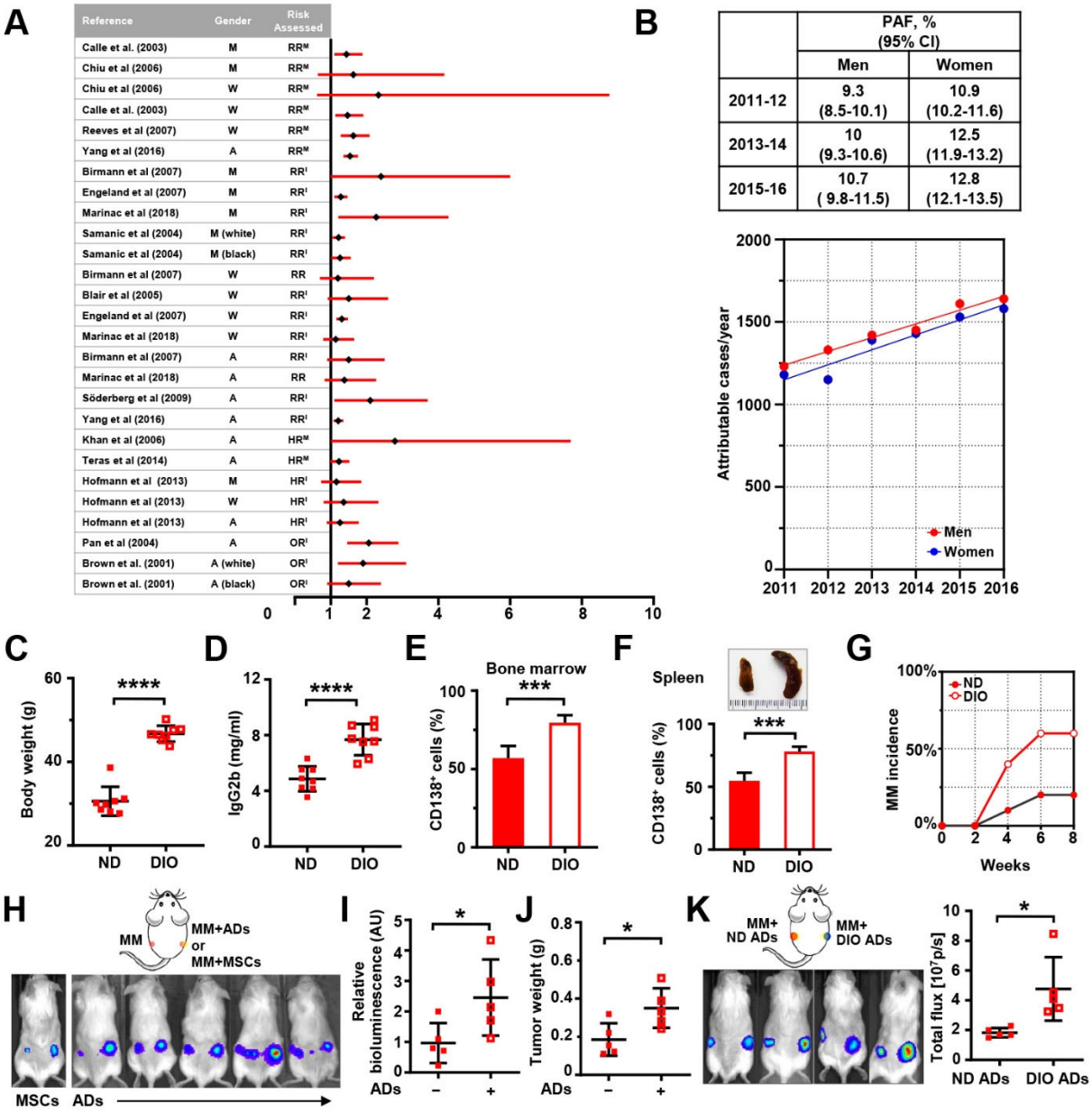

Figure S1. Association of obesity with multiple myeloma. Related to Figure 1. (A) A snapshot of the risk of obesity to myeloma from previous studies of single cohort or pooled data. Shown is the examined risk in the types of relative risk (RR), hazard rate (HR), or odd ratios (OR), along with its 95% confidence intervals (CI). The distinction of assessment from incidence (I) or mortality (M) are hyphenated next to the type of risk. Gender choices are men (M), women

(W), or all (A). (**B**) An estimated attributable risk as measured by percentage of population attributable fraction (PAF) and attributable cases to obesity from 2011 to 2016 in men or women of US. **(C-F)** Mouse body weights (C), levels of IgG2b in mouse sera (D), percentages of marrow-infiltrated $CD138^+$ myeloma cells (E), representative images of mouse spleens (upper) and percentages of spleen-infiltrated $CD138^+$ myeloma cells (lower, F) in C57BL/6J ND or DIO mice that were intrafemorally injected with Vk12598 cells (n=8/group). (**G**) Myeloma incidence rate in ND or DIO mice that were intravenously injected with myeloma 5TGM1 cells after 8 weeks (n=10/group). (**H-J**) Illustrated injection sites and representative images (H), summarized data of bioluminescent signals (I), and tumor weights (J) in NSG mice 4 weeks after subcutaneously injected with luciferase-labeled ARP-1 cells alone or mixed with MSCs or adipocytes. (**K**) Illustrated injection sites, representative images, and summarized data of bioluminescent signals in NSG mice 4 weeks after subcutaneously injected with luciferase-labeled ARP-1 cells mixed with adipocytes isolated from ND (ND ADs) or DIO mice (DIO ADs). Data shown as mean ± SD are representative of 3 independent experiments. **P*<0.05. ****P*<0.001. *****P*<0.0001. *P* values were determined by two-tailed Student's *t*-test.

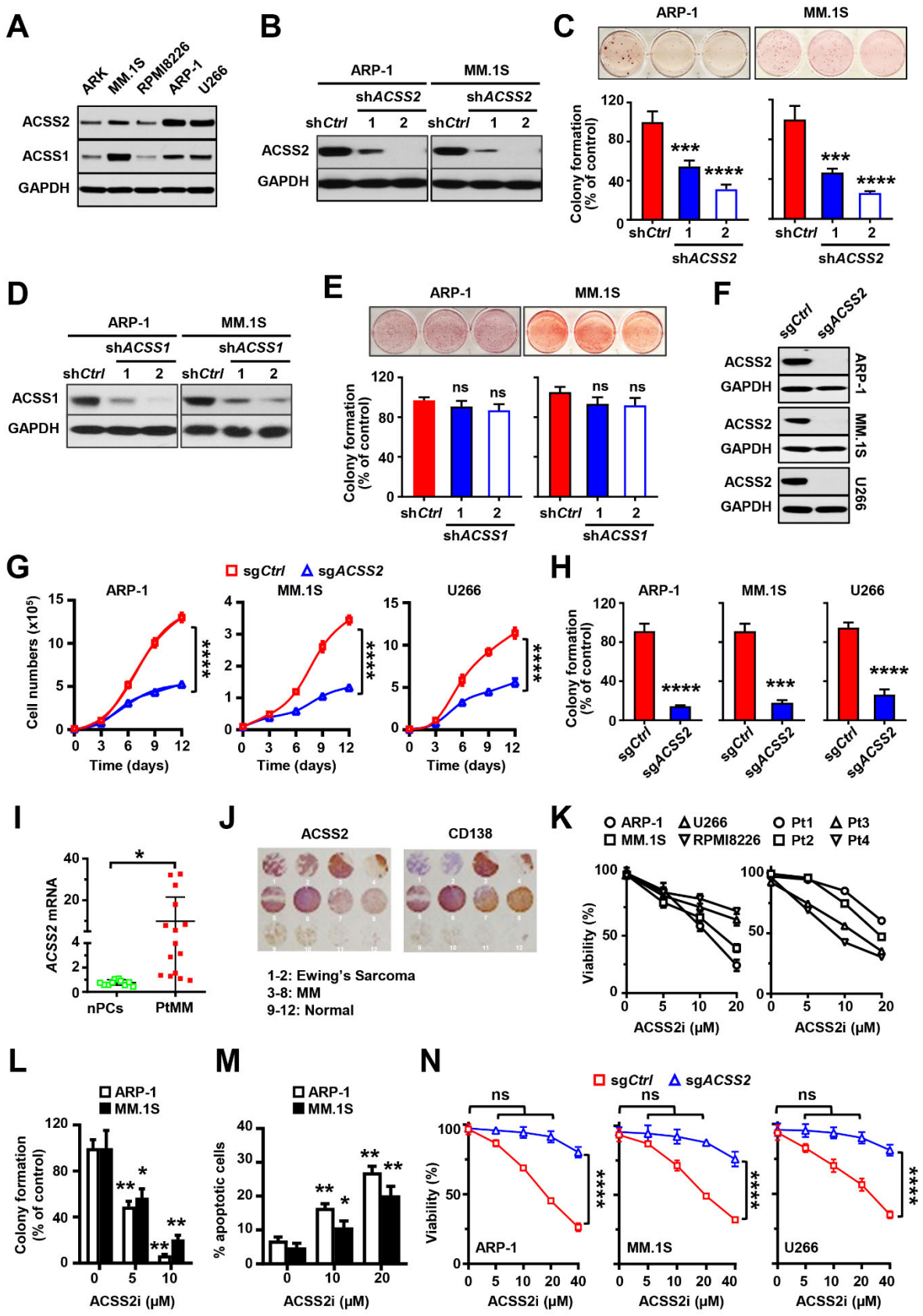
A
ARK
MM.1S
RPMI8226
ARP-1
U266
ACSS2
ACSS1
GAPDH
B
ARP-1
MM.1S
shACSS2
shCtrl
1
2
ACSS2
GAPDH
C
ARP-1
MM.1S
Colony formation (% of control)
***
****
shCtrl
shACSS2
D
ARP-1
MM.1S
shACSS1
ACSS1
GAPDH
E
ARP-1
MM.1S
Colony formation (% of control)
ns
shACSS1
F
sgCtrl
sgACSS2
ACSS2
GAPDH
ARP-1
MM.1S
U266
G
sgCtrl
sgACSS2
ARP-1
MM.1S
U266
Cell numbers (x10⁵)
Time (days)
****
H
ARP-1
MM.1S
U266
Colony formation (% of control)
I
ACSS2 mRNA
nPCs
PtMM
J
ACSS2
CD138
1-2: Ewing's Sarcoma
3-8: MM
9-12: Normal
K
ARP-1
U266
MM.1S
RPMI8226
Pt1
Pt2
Pt3
Pt4
Viability (%)
ACSS2i (μM)
L
ARP-1
MM.1S
Colony formation (% of control)
ACSS2i (μM)
M
ARP-1
MM.1S
% apoptotic cells
ACSS2i (μM)
N
sgCtrl
sgACSS2
ns
Viability (%)
ARP-1
MM.1S
U266
ACSS2i (μM)

Figure S2. The role of ACSS2 in myeloma growth *in vitro*. Related to Figures 2 and 3. (**A**) ACSS1 and ACSS2 protein levels in myeloma cell lines. (**B-E**) Myeloma cells were infected with lentivirus carrying non-targeted control (sh*Ctrl*) or two clones of short-hairpin RNAs against human *ACSS1* (sh*ACSS1*) or *ACSS2* (sh*ACSS2*). (**B, D**) Protein levels of ACSS2 (B) or ACSS1 (D) in myeloma cells. (**C, E**) Representative images of sh*ACSS2* (C) or sh*ACSS1* (E) myeloma cell colonies (upper) and summarized data for relative colony formation (lower). (**F**-**H**) Myeloma cell lines ARP-1, MM.1S, or U266 cells were infected with lentivirus carrying non-target control (sg*Ctrl*) or sequences encoding a guide RNA against *ACSS2* gene (sg*ACSS2*). (**F**) ACSS2 protein level in sg*Ctrl* and sg*ACSS2* myeloma cells. (**G**) Proliferation of sg*Ctrl* and sg*ACSS2* myeloma cells over time. (**H**) Colony formation of sg*Ctrl* or sg*ACSS2* myeloma cells. (**I**) Relative expression of *ACSS2* mRNAs in normal plasma cells from healthy donors (nPCs; n=11) or malignant plasma cells isolated from bone marrow aspirates of myeloma patients (PtMM; n=15). (**J**) Representative images of immunohistochemical staining show ACSS2 or CD138 expression in a tissue array containing bone marrow biopsy segments of myeloma patients (n=6), patients with Ewing's sarcoma (n=2; $CD138^{-}$ controls), and normal bone marrow biopsies (n=4). (**K**) Percentages of viability in human myeloma cell lines (left) and primary myeloma cells isolated from bone marrow aspirates of myeloma patients (n=4, right) 48 hours after treatment of ACSS2 inhibitor (ACSS2i). Cells without the treatment were set to 100%. (**L**) Colony formation of myeloma cells treated with indicated doses of ACSS2i. (**M**) Percentages of apoptotic cells in myeloma cells treated with indicated doses of ACSS2i. (**N**) Viability of myeloma cells expressing sg*Ctrl* or sg*ACSS2* after 48 hours of ACSS2i treatment. Data shown as mean ± SD are representative of 3 independent experiments. ns, not significant. *$P < 0.05$. **$P<0.01$. ***$P<0.001$. ****$P<0.0001$. *P* values were determined by two-tailed Student's *t*-test

(C, E, and H), one-way ANOVA with Newman-Keuls post hoc test (L, M) or two-way ANOVA with Bonferroni's post hoc test (G, N).

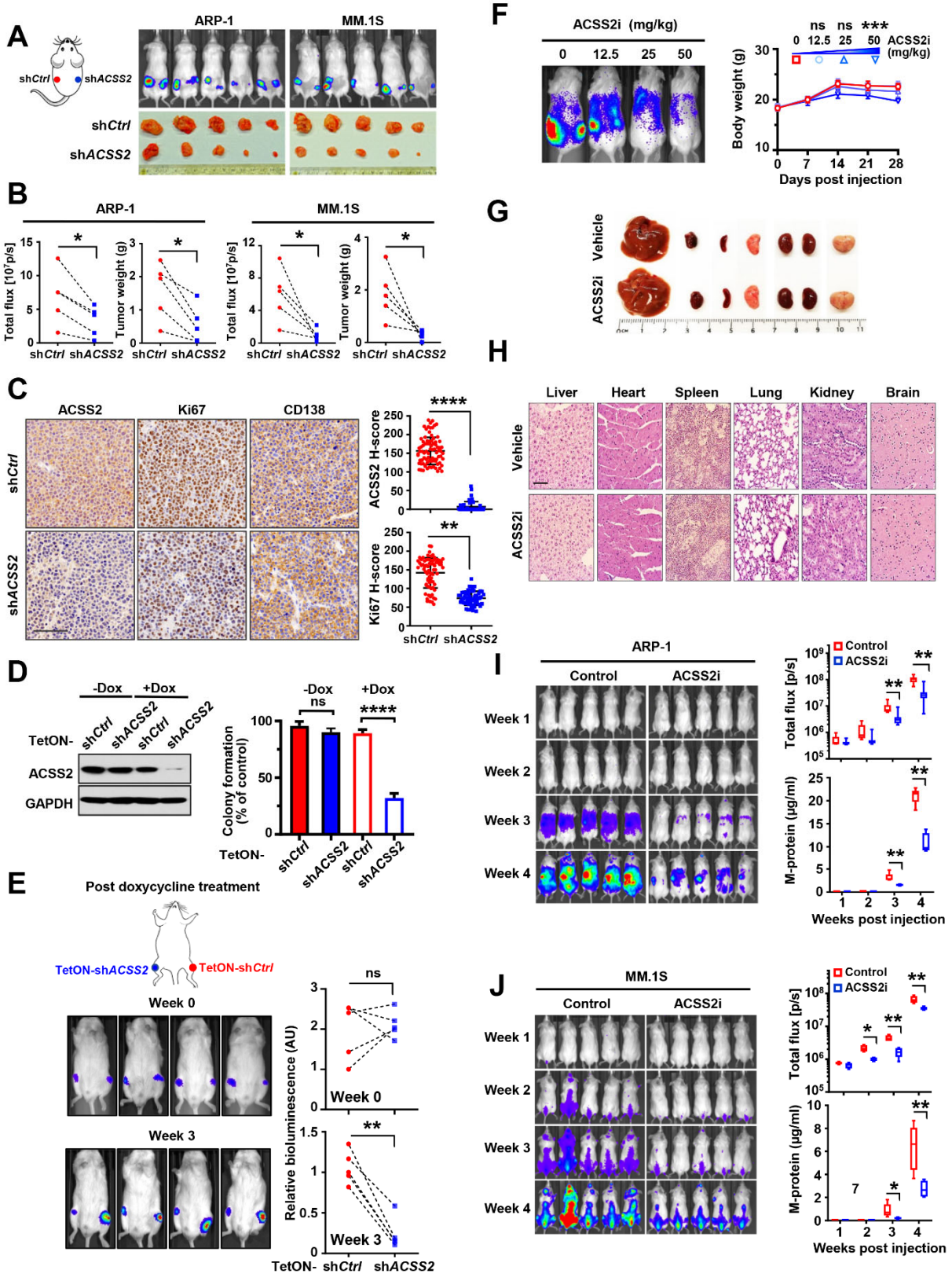
A
ARP-1
MM.1S
shCtrl
shACSS2
B
ARP-1
MM.1S
Total flux [10⁷p/s]
Tumor weight (g)
C
ACSS2
Ki67
CD138
ACSS2 H-score
Ki67 H-score
D
-Dox
+Dox
TetON-
ACSS2
GAPDH
Colony formation (% of control)
E
Post doxycycline treatment
TetON-shACSS2
TetON-shCtrl
Week 0
Week 3
Relative bioluminescence (AU)
F
ACSS2i (mg/kg)
Body weight (g)
Days post injection
G
Vehicle
ACSS2i
H
Liver
Heart
Spleen
Lung
Kidney
Brain
I
ARP-1
Control
Week 1
Week 2
Week 3
Week 4
Total flux [p/s]
M-protein (μg/ml)
Weeks post injection
J
MM.1S

Figure S3. ACSS2 promotes myeloma development *in vivo*. Related to Figures 2 and 3. (**A-C**) Luciferase-labeled sh*ACSS2* myeloma cells were subcutaneously injected into the right flank of NSG mice, while an equal number of sh*Ctrl* cells were injected into the left flank of the same mice. Shown are representative images (**A**) and summarized data (**B**) for bioluminescent signals and tumor weights after tumor cell implantation. (**C**) Immunohistochemical staining of ACSS2, Ki67, and CD138 expression in tumor tissues (left) and summarized data for ACSS2 and Ki67 (rights). Scale bar, 100 μm. (**D-E**) Luciferase-labeled ARP-1 cells were infected with lentivirus expressing a doxycycline-inducible *ACSS2* shRNA (TetON-sh*ACSS2*) or non-targeting control (TetON-sh*Ctrl*). (**D**) The protein expression of ACSS2 (left) and colony formation (right) of myeloma cells expressing TetON-sh*Ctrl* or TetON-sh*ACSS2* with or without doxycycline induction. (**E**) Schematic setting, representative bioluminescent images, and summarized data for bioluminescent signals of NSG mice that were intrafemorally injected with ARP-1 cells carrying inducible TetON-sh*Ctrl* or TetON-sh*ACSS2* at week 0 and 3 post-doxycycline treatment. (**F**) Shown are representative images of bioluminescent signals 3 weeks after ACSS2i treatment (left) and changes in mouse body weights (right) in NSG mice that were intravenously injected with luciferase-labeled ARP-1 cells and treated with various dosages of ACSS2i. (**G-H**) Representative images (G) and H&E staining (H) of vital organs from NSG mice treated with vehicle control or ACSS2i at 25 mg/kg dosage after 3 weeks. Scale bar, 100 μm. (**I-J**) Shown are representative images (left) and summarized data (right) of bioluminescent signals and serum M-protein levels in NSG mice that were intravenously injected with luciferase-labeled ARP-1 cells (**I**) or MM.1S cells (**J**) and treated with 25 mg/kg ACSS2i. Data shown as mean ± SD are representative of three independent experiments. ns, not significant. **P*<0.05, ***P*<0.01. ****P*<

0.001. ****$P < 0.0001$. *P* values were determined by two-tailed Student's *t*-test (B, C, and E) or two-way ANOVA with Bonferroni's multiple comparisons test (D, F, I, and J).

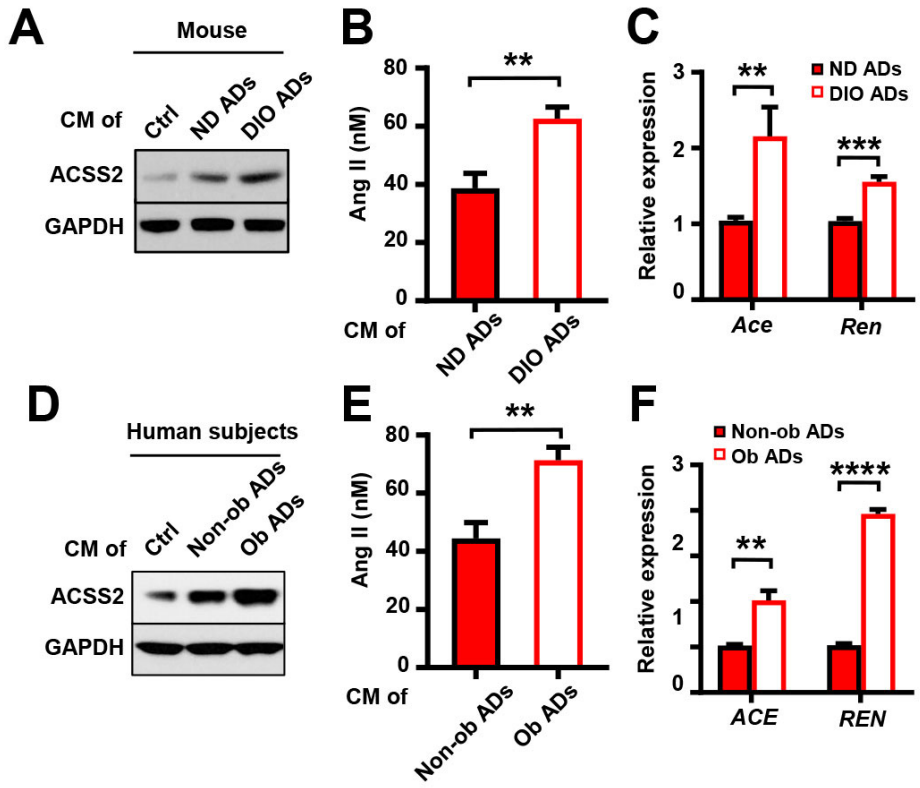

Figure S4. Adipocytes isolated from obese subjects produce more angiotensin II. Related to Figure 4. (**A-C**) Adipocytes isolated from visceral adipose tissue of ND (ND ADs) or DIO mice (DIO ADs) were cultured for 3 days to collect conditioned medium. (**A**) ACSS2 protein expression in ARP-1 cells cultured in the conditioned medium. (**B**) ELISA shows the concentration of angiotensin II in the conditioned medium. (**C**) Relative expression of *Ace* and *Ren* mRNAs in murine adipocytes. (**D-F**) Adipocytes isolated from visceral adipose tissue of human subject with obesity (Ob ADs) or with normal weight (Non-ob ADs) were cultured for 3 days to collect conditioned medium. (**D**) Expression of ACSS2 protein in ARP-1 cells cultured in the conditioned medium. (**E**) ELISA shows the concentration of angiotensin II in the conditioned medium. (**F**) Relative expression of *ACE* and *REN* mRNAs in adipocytes isolate from visceral adipose tissue of human subjects with obesity (Ob ADs) or with normal weight (Non-ob ADs).

Data shown as mean ± SD are representative of three independent experiments. **P<0.01. ****P< 0.0001. P values were determined by two-tailed Student's t-test.

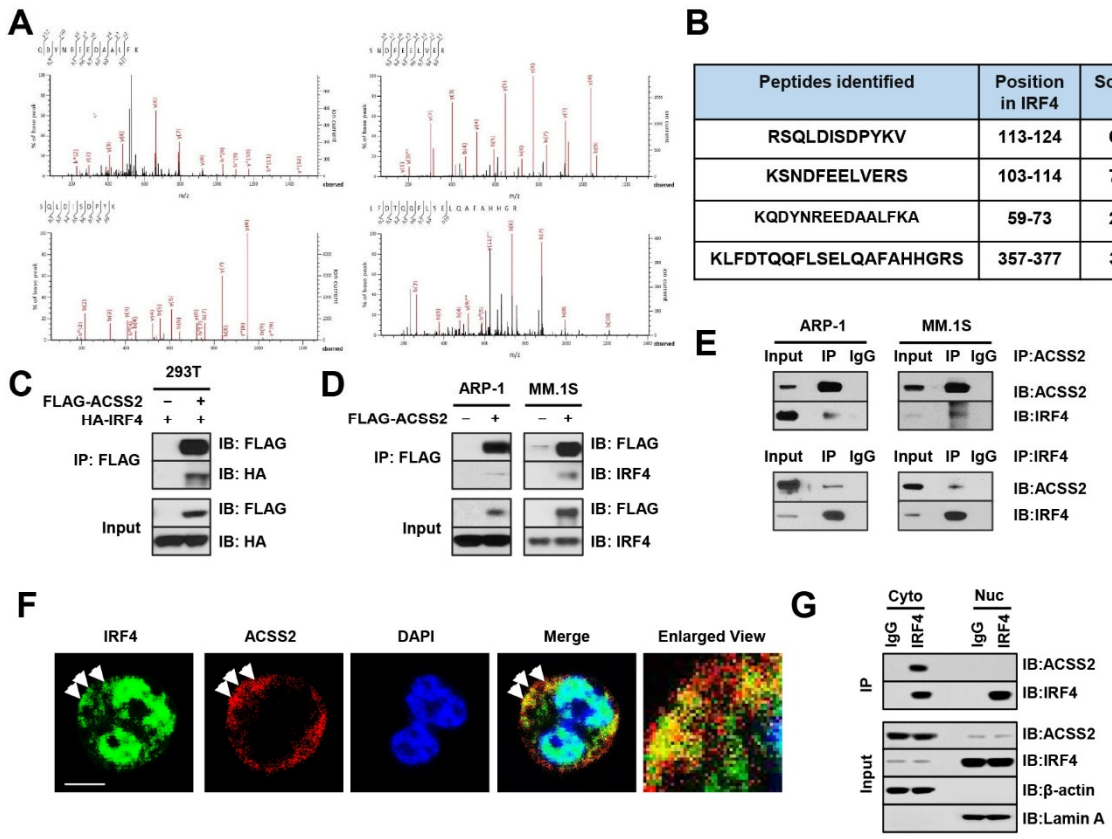

Figure S5. Identification of the oncogenic protein IRF4 that interacts with ACSS2. Related to Figure 5. (**A)** Mass spectrometry analysis of immunoprecipitates pulled down by anti-FLAG resin from ARP-1 cells infected with lentivirus carrying FLAG-tagged ACSS2. Cells infected with empty vector served as control. (**B**) List of identified peptides matching the sequence of IRF4 protein from mass spectrometry. (**C**) Co-immunoprecipitation of HA-tagged *IRF4* (HA-*IRF4*) and FLAG-tagged *ACSS2* (FLAG-*ACSS2*) in HEK293T cells. Cells co-transfected with FLAG-*ACSS2* and HA-*IRF4* were immunoprecipitated with anti-FLAG resin and immunoblotted with anti-HA or anti-FLAG antibodies. Cells transfected with HA-*IRF4* and FLAG-tagged control vector served as controls. (**D**) Immunoprecipitation of ARP-1 or MM.1S cells infected with lentivirus carrying FLAG-*ACSS2* or empty vector control. Cell lysates were immunoprecipitated with anti-FLAG resin and immunoblotted against anti-FLAG and anti-IRF4

antibodies. (**E**) Immunoprecipitation of ARP-1 or MM.1S cell lysates using antibody against ACSS2 or IRF4 to detect endogenous ACSS2-IRF4 interaction. The immunoprecipitates were immunoblotted with anti-ACSS2 and anti-IRF4 antibodies. (**F**) Representative immunofluorescent graphs of myeloma ARP-1 cells stained with DAPI and antibodies against IRF4 or ACSS2. Arrows: co-location of ACSS2 and IRF4 proteins. Scale bar, 10 μm. (**G**) Immunoprecipitation of cytoplasmic or nuclear fractions of ARP-1 cells using the antibody against IRF4. The immunoprecipitates were immunoblotted with anti-ACSS2 or anti-IRF4 antibodies. Immunoglobulin G (IgG) was used as control, and lysates from cytoplasmic or nuclear fractions were used as input control. Immunoblotting with β-actin was used as cytosolic marker; immunoblotting with lamin A was used as nuclear marker.

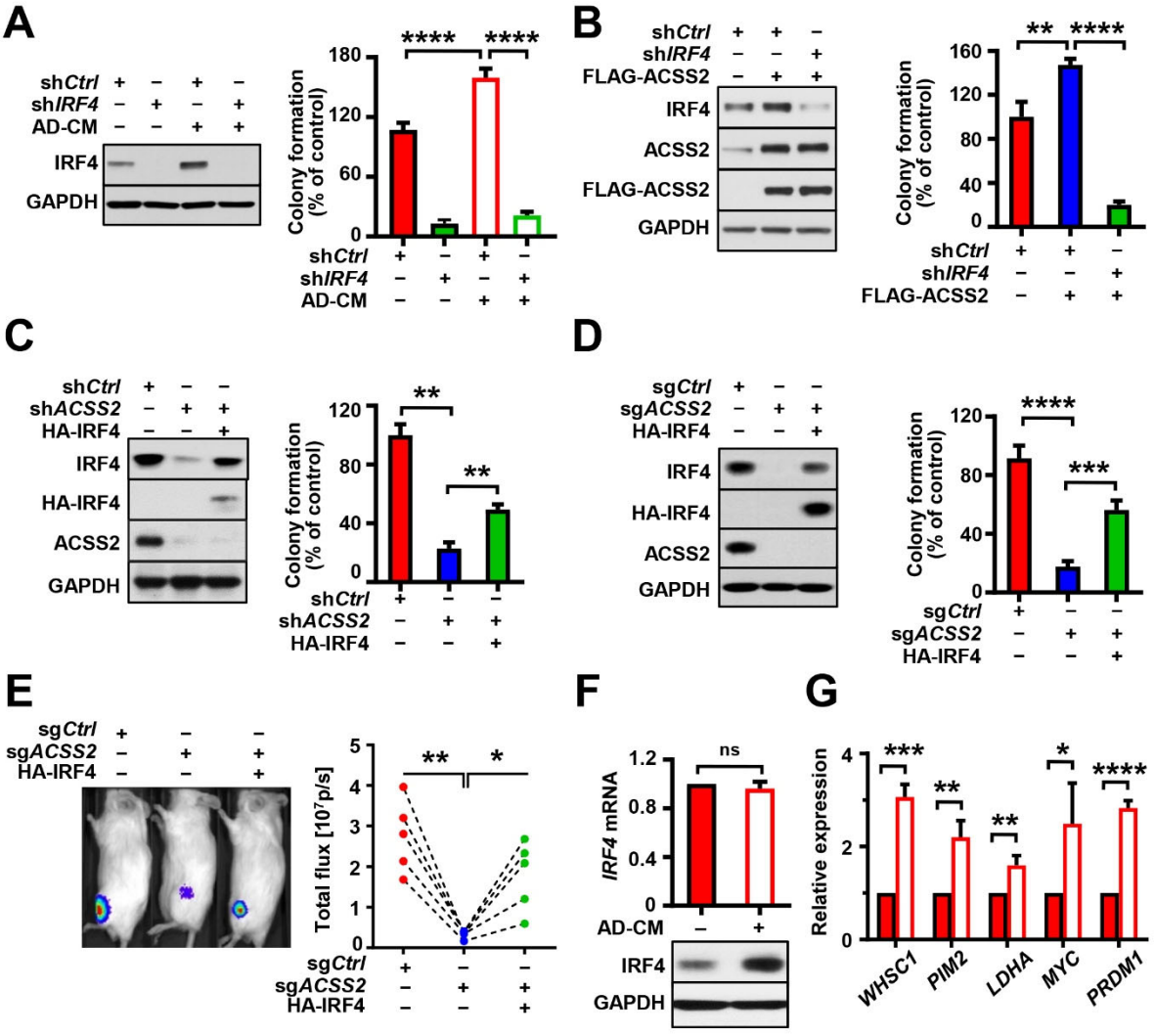

Figure S6. IRF4 is implicated in adipocyte-enhanced myeloma tumorigenesis. Related to Figure 5. (**A**) IRF4 protein (left) and colony formation (right) in sh*IRF4*-expressing ARP-1 cells that were cultured in adipocyte conditioned medium (AD-CM). (**B**) Protein levels of IRF4, ACSS2, and FLAG-ACSS2 (left) and colony formation (right) in FLAG-ACSS2–expressing ARP-1 cells that were infected with lentivirus carrying sh*Ctrl* or sh*IRF4*. (**C**) Protein levels of IRF4, HA-tagged IRF4 (HA-IRF4), and ACSS2 (left) and colony formation (right) in sh*ACSS2*-expressing ARP-1 cells that were infected with lentivirus carrying HA-tagged IRF4 or empty control. (**D-E**) Luciferase-labeled MM.1S cells expressing sg*Ctrl* or sg*ACSS2* were infected with

lentivirus carrying HA-IRF4 or empty vector control. (D) Protein levels of IRF4, HA-IRF4, and ACSS2 (left) and colony formation (right). (E) Representative images of bioluminescent signals (left) and summarized data for the relative bioluminescent signals (right) in NSG mice 3 weeks after intrafemoral injection with myeloma cells. (**F-G**) The mRNA and protein levels of IRF4 (F) and relative expression of *WHSC1*, *PIM2*, *LDHA*, *MYC*, and *PRDM1* mRNAs (G) in ARP-1 cells that were cultured in AD-CM for 24 hours. Data shown as mean ± SD are representative of 3 independent experiments. ns, not significant. **P*<0.05. ***P*<0.01. ****P*<0.001. *****P*< 0.0001. P values were determined by two-tailed Student's *t*-test (F, G), one-way ANOVA with Bonferroni's post hoc test (B-E) or two-way ANOVA with Bonferroni's post hoc test (A).

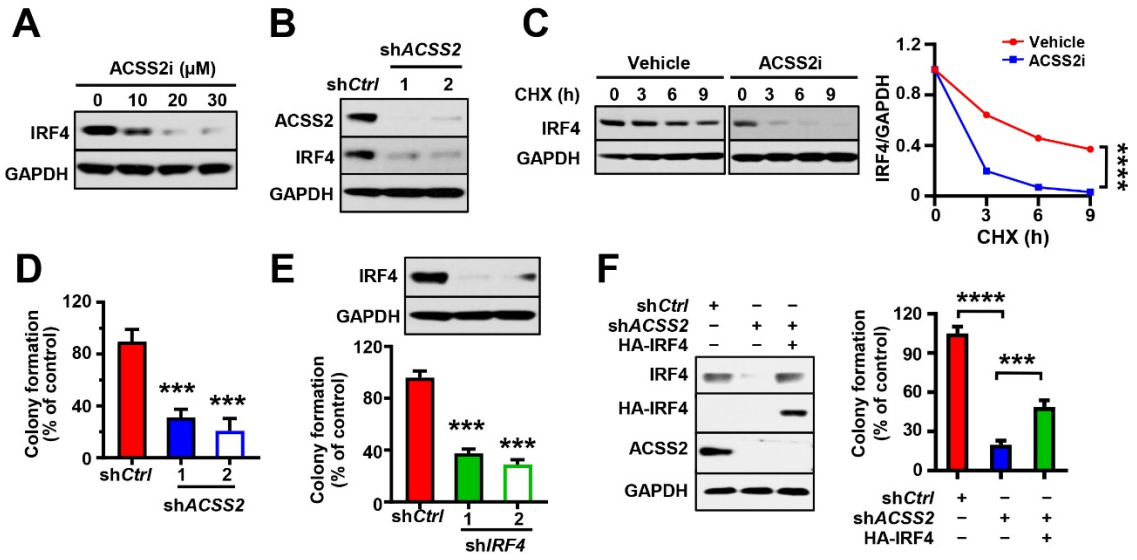

Figure S7. ACSS2 enhances IRF4 stability and tumor growth in melanoma. Related to Figure 5. (**A-B**) IRF4 protein level in human melanoma A375 cells treated with various concentrations of ACSS2i for 24 hours (A) or A375 cells carrying non-target control shRNA (sh*Ctrl*) or shRNA targeting ACSS2 (sh*ACSS2;* B). (**C**) Time course in hours (h) of IRF4 protein levels in A375 cells treated with 10 μM ACSS2i and 100 μM cycloheximide (CHX). Right: normalized IRF4 levels against GAPDH. (**D**) Colony formation assay shows the summarized data from A375 cells carrying sh*Ctrl* or one of the two clones of sh*ACSS2*. (**E**) IRF4 protein level (upper) and soft agar growth (lower) of A375 cells carrying sh*Ctrl* or one of the two clones of shRNA targeting IRF4 (sh*IRF4)*. (**F**) IRF4, HA-IRF4, and ACSS2 protein levels (left) and relative colony formation (right) in sh*ACSS2*-expressing A375 cells that were infected with lentivirus encoding HA-IRF4 or empty control. Data shown as mean ± SD are representative of 3 independent experiments. ***P<0.001. ****P< 0.0001. P values were determined by two-tailed Student's t- test (D, E), one-way ANOVA with Newman-Keuls post hoc test (F), or two-way ANOVA with Bonferroni's post hoc test (C).

Supplementary Tables

Table S1. Summarized characteristics of myeloma patients with normal weight, overweight, or obesity. Related to Figures 1 and 7, and STAR Methods.

Average (Range)			
	Normal (n=11)	Overweight (n=9)	Obese (n=11)
Age	66.2 (50-84)	56.1 (42-70)	64.8 (51-90)
Male	54.5%	44.4%	54.5%
Female	45.5%	55.6%	45.5%
BMI	22.7 (20.8-24.4)	26.2 (25.1-28.4)	32.4 (30-35.9)
Disease Status	Newly diagnosed MM	Newly diagnosed MM	Newly diagnosed MM
Bone lesion	70.0%*	88.89%	81.82%

*Several cases have missing information.

Table S2. Primers for real-time RT-PCR analysis. Related to STAR Methods.

Gene	Forward	Reverse
ACSS2	TTGGGGCCTTTGCACTCCATT	AGGCATCTGTAGTGATGAGAAGA
IRF4	CCTACACCATGACAACGCCT	CTGTCACCTGGCAACCATTT
AGTR1	ATTTAGCACTGGCTGACTTATGC	CAGCGGTATTCCATAGCTGTG
AGTR2	AAACCGGTTCCAACAGAAGC	GAGCCTCAAAGCAAGTAGCC
WHSC1	CCTCCAACAGCATCATCTGC	CGTCAGGCATCTCGATGTTC
PIM2	GCTATGGAAAGTGGGTGCAG	ATGAAGCCCTCCTGTGTCTC
LDHA	ATGGCAACTCTAAAGGATCAGC	CCAACCCCAACAACTGTAATCT
MYC	CTGCGACGAGGAGGAGAA	CCGAAGGGAGAAGGGTGT
PRDM1	AAGCAACTGGATGCGCTATGT	GGGATGGGCTTAATGGTGTAGAA
ACE	GGAGGAATATGACCGGACATCC	TGGTTGGCTATTTGCATGTTCTT
REN	ACCTTTGGTCTCCCGACAGA	CACCTCGTTCCTTCAGGCTTT
GAPDH	GCACCGTCAAGGCTGAGAAC	TGGTGAAGACGCCAGTGGA
Irf4	TCCGACAGTGGTTGATCGAC	CCTCACGATTGTAGTCCTGCTT
Acss2	AAACACGCTCAGGGAAAATCA	ACCGTAGATGTATCCCCCAGG
Whsc1	TGCCAAAAAGGAGTACGTGTG	CTTCGGGAAAGTCCAAGGCAG
Myc	CCGCCCTTTATATTCCGGGG	CCTTCTTTTTCCCGCCAAGC
Pim2	CACGGATAGACGTCAGGTGG	AAACCAGTCAAGCAGGCGTA
Ldha	TGTCTCCAGCAAAGACTACTGT	GACTGTACTTGACAATGTTGGGA
Prdm1	TTCTCTTGGAAAAACGTGTGGG	GGAGCCGGAGCTAGACTTG
Ace	AGGTTGGGCTACTCCAGGAC	GGTGAGTTGTTGTCTGGCTTC
Ren	CTCTCTGGGCACTCTTGTTGC	GGGAGGTAAGATTGGTCAAGGA
Gapdh	AGGTCGGTGTGAACGGATTTG	TGTAGACCATGTAGTTGAGGTCA

Table S3. Primers used in subcloning of short-hairpin RNA into the pLKO.1 vector. Related to STAR Methods.

shRNA	Direction	Sequence
sh*ACSS1*-1	Forward	CCGGCTGTTGCTGAAATACGGTGATCTCGAGATCACCGTATTTCAGCAACAGTTTTTG
	Reverse	AATTCAAAAACTGTTGCTGAAATACGGTGATCTCGAGATCACCGTATTTCAGCAACAG
sh*ACSS1*-2	Forward	CCGGCCAGTTAAATGTCTCTGTCAACTCGAGTTGACAGAGACATTTAACTGGTTTTTG
	Reverse	AATTCAAAAACCAGTTAAATGTCTCTGTCAACTCGAGTTGACAGAGACATTTAACTGG
sh*ACSS2*-1	Forward	CCGGGCTTCTGTTCTGGGTCTGAATCTCGAGATTCAGACCCAGAACAGAAGCTTTTTG
	Reverse	AATTCAAAAAGCTTCTGTTCTGGGTCTGAATCTCGAGATTCAGACCCAGAACAGAAGC
sh*ACSS2*-2	Forward	CCGGCGGTTCTGCTACTTTCCCATTCTCGAGAATGGGAAAGTAGCAGAACCGTTTTTG
	Reverse	AATTCAAAAACGGTTCTGCTACTTTCCCATTCTCGAGAATGGGAAAGTAGCAGAACCG
sh*IRF4*	Forward	CCGGTTTACTGAAATGCGCTCTTTACTCGAGTAAAGAGCGCATTTCAGTAAATTTTTG
	Reverse	AATTCAAAAATTTACTGAAATGCGCTCTTTACTCGAGTAAAGAGCGCATTTCAGTAAA
sh*p62*-1	Forward	CCGGGCAGATGAGAAAGATCGCCTTCTCGAGAAGGCGATCTTTCTCATCTGCTTTTTG
	Reverse	AATTCAAAAAGCAGATGAGAAAGATCGCCTTCTCGAGAAGGCGATCTTTCTCATCTGC
sh*p62*-2	Forward	CCGGGCCCTCCATTTGTAAGAACAACTCGAGTTGTTCTTACAAATGGAGGGCTTTTTG
	Reverse	AATTCAAAAAGCCCTCCATTTGTAAGAACAACTCGAGTTGTTCTTACAAATGGAGGGC
sh*Ctrl*	Forward	CCGGCCTAAGGTTAAGTCGCCCTCGCTCGAGCGAGGGCGACTTAACCTTAGGTTTTTG
	Reverse	AATTCAAAAACCTAAGGTTAAGTCGCCCTCGCTCGAGCGAGGGCGACTTAACCTTAGG

Table S4. Primers used in subcloning of single-guide RNA into the lentiCRISPRv2 vector. Related to STAR Methods.

sgRNA	Direction	Sequence
sg*ACSS2*	Forward	CACCGATTCTGGGGAGACATTGCCA
	Reverse	TTTGACCGTTACAGAGGGGTCTTAG
sg*Ctrl*	Forward	CACCGCCAGGCTGAAGTTCGTACCT
	Reverse	TTTGTCCATGCTTGAAGTCGGACCG

Table S5. Primers used in ChIP assay. Related to STAR Methods.

Genes	Direction	Sequence
PRDM1	Forward	GGACAGAGGCTGAGTTTGAAGA
	Reverse	CGCCATCAGCACCAGAATC
MYC	Forward	GAACGCGCGCCCATTAATAC
	Reverse	CTCGCTAAGGCTGGGGAAAG
PIM2	Forward	TCTCAACTCCAAGAGCAGCC
	Reverse	GGGAACCCCTACCATCAACG
LDHA	Forward	GAGATGAGATGCCAGTGGGG
	Reverse	TTTCCCTCTGCTGCTAAGCC
WHSC1	Forward	GGACTCGTTCACGCCCTG
	Reverse	GAGAGGGTCAGACGCCACG